Journal of Power Sources 195 (2010) 327–334

Contents lists available at ScienceDirect

Journal of Power Sources

journal homepage: www.elsevier.com/locate/jpowsour

Interface-mediated electrochemical effects in lithium/polymer-ceramic cells

Jitendra Kumar[a,*], Stanley J. Rodrigues[b], Binod Kumar[a]

[a] Electrochemical Power Group, Metals & Ceramics Division, University of Dayton Research Institute, Dayton, Ohio 45469-0171, USA
[b] Air Force Research Laboratory, Propulsion Directorate, WPAFB, Ohio 45433, USA

ARTICLE INFO

Article history:
Received 15 June 2009
Received in revised form 29 June 2009
Accepted 30 June 2009
Available online 8 July 2009

Keywords:
Polymer-ceramic composite
Ionic transport
Charge-transfer reaction
Solid electrolyte interface

ABSTRACT

The paper presents and discusses a method to achieve beneficial electrochemical effects mediated by interfaces in an ionic conducting polymer matrix. The beneficial effects include enhanced ionic transport, catalysis of anodic oxidation reaction, and stabilization of the lithium-electrolyte interface in lithium-based electrochemical cells. Polyethylene oxide (PEO) doped with $LiN(SO_2CF_2CF_3)_2$ (LiBETI) was chosen as the ion conducting polymer matrix. The polymer-ceramic (PC) composite electrolytes from the PEO:LiBETI-BN and PEO:LiBETI-Li_2O systems were optimized to achieve high conductivity, reduce charge-transfer resistance, and stabilize the solid electrolyte interface (SEI) layer at the lithium anode. Both BN and Li_2O were effective in enhancing interface-mediated lithium ion transport. The charge-transfer resistance was reduced by orders of magnitude and the long-term stability of the cells was improved remarkably due to the addition of BN and Li_2O in the PEO:LiBETI polymer matrix. AC impedance spectroscopy was used to investigate the phenomenon by measuring the time- and temperature-dependent electrical behavior of the aforementioned materials and cells. The interface-mediated effects due to the addition of BN and Li_2O dielectrics contributed to the improved cell properties.

Published by Elsevier B.V.

1. Introduction

The term interface-mediated refers to an accumulation of local, uncompensated charges in bulk solids. The charges may result from the ionization and adsorption of species at interfaces and/or on dielectric surfaces. These charges may have a major influence on the electrical properties of solids and the electrochemical devices fabricated from those solids.

The first demonstration of the interface-mediated ionic transport may be traced to the work of Liang [1]. In the pioneering paper, Liang [1] reported that lithium iodide (LiI) doped with 35–45 mol% of aluminum oxide enhanced conductivity by almost a factor of 50 at 25 °C. However, the amount of aluminum oxide determined to be soluble in LiI was insignificant. Subsequently, a number of investigators have reported enhanced conductivity of silver in the AgI–Al_2O_3 system [2], copper in the CuCl–Al_2O_3 system [3], fluorine in the PbF_2–SiO_2 and PbF_2–Al_2O_3 systems [4] and lithium in polymer-ceramic composite electrolytes [5]. Three review papers [6–8] also document the developmental history and general properties of theses heterogeneous ionic conductors.

The oxidation of lithium at the lithium electrode and the transport of lithium ions through the electrolyte are the fundamental electrochemical processes that take place in lithium-based electrochemical cells. The performance of these cells primarily depends upon the kinetics of the two processes. The slowest process determines the performance of the cells. With a recent surge in interest in lithium-based electrochemical cells, it has become imperative that materials be developed to enhance the kinetics of both processes.

Composite membranes are heterogeneous solid ionic conductors in which a dielectric phase is dispersed by design. Prior publications [9–11] have reported the effects of the dielectric phase on the ionic conductivity in terms of the space charge and blocking effects in the composite membranes. The ionic conductivity of the composite membranes is of profound interest to chemists and engineers because of its application in commercial electrochemical devices such as batteries, fuel cells, electrolyzers, electrosynthesizers, and sensors. The requirements of these electrochemical devices continue to evolve, and it is believed that the next generation of these devices will require electrolytes with a much higher conductivity in a wider temperature range.

The power sources based on lithium chemistry have been of considerable interest due to their high energy and power densities. The lithium–oxygen/air cell is perhaps the ultimate power source among the cells derived from lithium chemistry. However, its development has been impeded by the lack of suitable membranes. This paper will present and discuss some of the potential membrane materials for the lithium-composite solid electrolyte cells. The potential of these materials lies in the high ionic conductivity and improved stability of lithium-electrolyte interface of all solid electrochemical cells.

* Corresponding author. Tel.: +1 937 229 5314; fax: +1 937 229 3433.
E-mail address: kumarjit@notes.udayton.edu (J. Kumar).

0378-7753/$ – see front matter. Published by Elsevier B.V.
doi:10.1016/j.jpowsour.2009.06.098

2. Experimental

2.1. Processing of polymer-ceramic membranes

As-received poly(ethylene)oxide (PEO) (M.W. 2,000,000 Union Carbide) and $LiN(SO_2CF_2CF_3)_2$ (3 M), hereafter called LiBETI, were used as solvent and solute, respectively, to prepare a polymer electrolyte. The PEO and LiBETI were dried in an oven at 50 and 60 °C, respectively, for 48 h. The PEO:LiBETI (8.5:1) electrolyte was prepared by an energy milling technique which is a solvent-free process. The chemicals were weighed inside a glove box maintained at <50 ppm of O_2 and <88 ppm of H_2O. The batch was contained in an airtight metallic jar and subsequently mixed using an energy mill (Spex Certi Pep 8000D mixer/mill; USA) for 1 h without a SS ball. Following the milling, 300 mg of the milled material was loaded into a preheated die (≈100 °C), and then pressed with 490 MPa pressure into a disc. Thus, specimens in the form of discs of 0.06–0.07 cm thickness and 1.27 cm diameter were obtained for characterization. All the specimens appeared transparent and rubbery after removal from the press. Composites of PEO:LiBETI (8.5:1)-BN(1 wt%) and PEO:LiBETI (8.5:1)-Li_2O(1 wt%) were also prepared using a similar procedure. The PEO:LiBETI (8.5:1)-BN/Li_2O will be referred to as the PC electrolyte and the ceramic phase will be identified by the chemical formula within parentheses such as PC(BN) and PC(Li_2O). Both nanosize BN (5–20 nm) and Li_2O powder were obtained from Alfa Aesar (30 Bond Street, Ward Hill, MA, USA) and used as-received.

2.2. Electrical conductivity measurement

AC impedance measurements on the specimens were carried out using a Solartron instrument (Model 1260 with an electrochemical interface; Solartron US, Houston TX) in the 0.1–10^6 Hz frequency range. The specimens were placed into a cell using SS or lithium as electrodes in a cell fixture. The fixture containing the cell was subsequently placed in a holder with attached electrical wires leading to the impedance spectrometer. The AC impedance of the cells was measured in the appropriate temperature range. At each temperature, the specimen was equilibrated for 1 h before the impedance measurement. AC impedance of the cells was also measured periodically for more than 1000 h of storage at ambient temperature. The *Z* Plot and *Z* View software packages were employed for data acquisition and analysis. The cell conductivity was computed from their AC impedance spectra and geometrical dimensions. The lithium ion transport number (t_{Li+}) of the electrolyte was measured on Li/electrolyte/Li symmetrical cell polarized by 0.1 V dc voltage. The Li/electrolyte interfacial and electrolyte bulk resistances (obtained by AC impedance spectra) and the currents were used to solve the expression for t_{Li+} as expressed by Eq. (i) below:

$$t_{Li^+} = \frac{[I_S R_{b(S)}(V - I_0 R_{i(0)})]}{[I_0 R_{b(0)}(V - I_S R_{i(S)})]} \quad \text{(i)}$$

where I_0 = initial current, I_S = current after application of dc voltage (V = 0.1 V) for 20 min, $R_{b(0)}$ and $R_{b(S)}$ bulk resistance before and after polarization respectively, $R_{i(0)}$ and $R_{i(S)}$ interface resistance before and after polarization respectively.

3. Results and discussions

The membranes were characterized by an AC impedance spectrometer using blocking, SS, and non-blocking lithium electrodes. The impedance data from these cells will initially be presented and analyzed independently. Subsequently, observations from both techniques will be synthesized to develop a comprehensive view on the transport mechanism, charge-transfer reaction, and stability of the SEI layer. These electrolytes are being evaluated for their use in lithium–oxygen/air cells. PC specimens containing range of weight fractions (0–5 wt%) of ceramic phases Li_2O and BN were evaluated. The specimens containing 1 wt% Li_2O and BN provided the desirable effects in terms of cell conductivity and stability. The data and discussions in the paper will be limited to PCs containing only 1 wt% of Li_2O and BN as investigations related to other wt% of Li_2O and BN are still under investigation. Fully rechargeable lithium-air cells using these electrolytes have been reported earlier [12,13] and will not be covered in this paper.

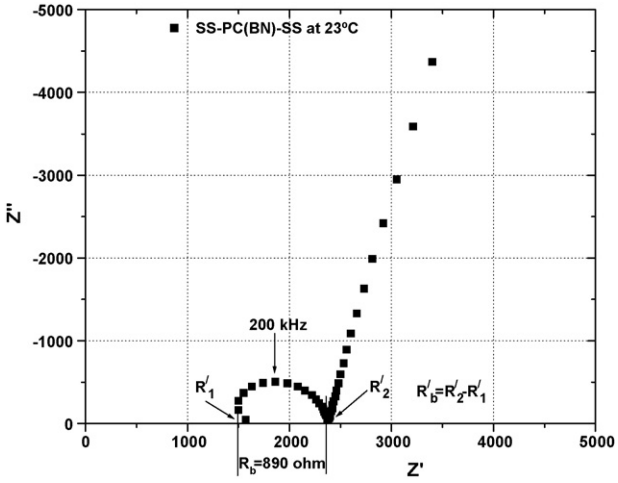

Fig. 1. Nyquist plot of PC(BN) an electrolyte using blocking electrodes (SS) at 23 °C.

3.1. Conductivity of electrolytes with blocking (SS) electrodes

A typical AC impedance spectra of SS/PC(BN)/SS electrolyte at room temperature in the form of the Nyquist plot is shown in Fig. 1. The spectra show two intersections (R'_1 and R'_2) at the Z′ axis forming a semicircle. The first intersection (R'_1) is interpreted as circuit resistance external to the specimen and it is related to electrolyte–electrode interface contact resistance. The distance between first (R'_1) and second (R'_2) intersections is interpreted as bulk electrolyte resistance ($R'_b = R'_2 - R'_1$). The R'_b at a particular temperature is further normalized with respect to the thickness and cross-sectional area to obtain the specimen conductivity. Similar AC impedance spectra were observed for SS/PEO:LiBETI/SS and SS/PC(Li_2O)/SS specimens.

The conductivity plots of PEO:LiBETI (8.5:1), PC(BN) and PC(Li_2O) specimens as measured with the blocking SS electrodes are shown in Fig. 2(a–c). All three plots show an inflection point around 68 °C. This is typical of the PEO-based electrolytes in which melting of the crystalline phase occurs around 68 °C. The linear regions above and below the inflection point show Arrhenius type behavior as expressed by Eq. (ii)

$$\sigma = \sigma_0 e^{-E_a/RT} \quad \text{(ii)}$$

where, σ = conductivity, σ_0 = pre exponential factor, E_a = activation energy, R = gas constant and T = temperature.

The specimens at temperature above 65 °C exhibit liquid-like conductivity with an activation energy of 0.36, 0.36, and 0.35 eV mol^{-1} for the PEO:LiBETI, PC(Li_2O), and PC(BN) electrolytes, respectively. At temperatures below 65 °C, the specimens display solid-like conductivity with activation energies of 1.15, 1.12, and 1.52 eV mol^{-1} for the PEO:LiBETI, PC(Li_2O), and PC(BN) electrolytes, respectively. The activation energies are comparable to the values reported by an earlier investigation [18].

The PC(BN) specimen shows higher conductivity—by about a factor of 2–3 below 65 °C and by a factor of 6–7 above 65 °C as com-

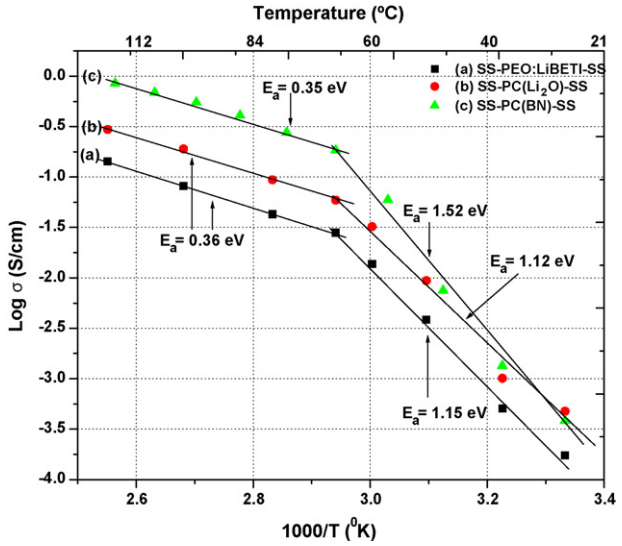

Fig. 2. Arrhenius plots (conductivity vs. temperature) of the PEO:LiBETI (8.5:1), PC(BN) and PC(Li_2O) electrolytes.

pared to the PEO:LiBETI (8.5:1) polymer specimen. The PC(Li_2O) specimen below 65 °C shows conductivity values between the PC(BN) and PEO:LiBETI (8.5:1) polymer specimens. The enhanced conductivity in both specimens, PC(BN) and PC(Li_2O), is attributed to the interface-mediated transport of ions. Fig. 2 suggests that the effect remains operative across the entire temperature range from 25 to 120 °C. In fact, the effect is more prominent in the liquid state (60–120 °C) than in the solid-state (25–60 °C), Fig. 2. The effect of the ceramic additive at lower temperatures (<65 °C) is similar to other additives such as Al_2O_3, $BaTiO_3$, and MgO in PEO-based electrolytes [5]. However, the effect at higher temperature (>65 °C) is far more prominent and desirable for BN and Li_2O additives as compared to the Al_2O_3, $BaTiO_3$, MgO [5].

The interface-mediated ionic transport is schematically shown in Fig. 3. The conducting ions, either lithium cation (Li^+) or $BETI^-$ anion ($N(SO_2CF_2CF_3)_2$), are represented by arrows, whereas the BN/Li_2O particles are depicted by solid circles. The background is a matrix composed of the PEO:LiBETI polymer. Some of the conducting ions interact with BN and attach to the BN dispersant to form a BN:Li^+/$BETI^-$ complex [14] as expressed by Eq. (iii).

$$BN + Li^+/BETI^- \Leftrightarrow BN : Li^+/BETI^- \quad \text{(iii)}$$

The BN:Li^+/$BETI^-$ complex becomes a source of local electric fields as illustrated by the arcs around the attached arrows in Fig. 3. The local electric field accelerates transport of the remaining conducting ions.

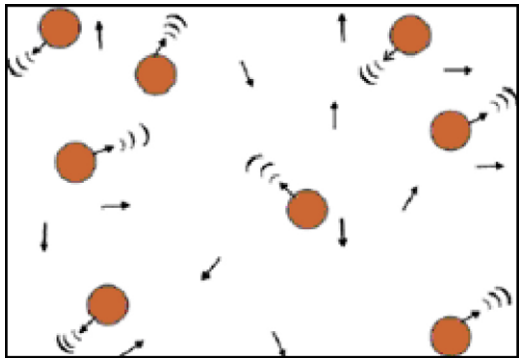

Fig. 3. Schematic representation of the interface-mediated interaction of ions (either cation or anion) with BN/Li_2O dielectrics in the PEO:LiBETI(8.5:1) polymer electrolyte matrix.

A similar chemical interaction is also being proposed for electrolyte with Li_2O dispersant. A significant number of Li^+ ions accumulate on and interact with Li_2O particles, and attach to Li_2O dispersant to form Li_2O:Li^+/$BETI^-$ complex (as the H_2O molecule does with H^+ ion) [14] as expressed by Eq. (iv).

$$Li_2O + Li^+/BETI^- \Leftrightarrow Li_2O : Li^+/BETI^- \quad \text{(iv)}$$

The Li_2O:Li^+/$BETI^-$ complex also becomes a source of local electric fields as illustrated by the arcs around the attached arrows in Fig. 3. This local electric field acts as an internal electric field amplifier that accelerates transport of the remaining conducting ions.

The transport number of lithium ion in the PC(BN) electrolyte (t_{Li+}) has been measured by using Eq. (i) as suggested by Abraham et.al. [15]. The t_{Li+} was determined to be 0.49 at room temperature.

Eqs. (iii) and (iv) also imply reversibility. A reversibility of the chemical processes similar to the one expressed by Eqs. (iii) and (iv) in another ionic conductor-dielectric heterogeneous system has been reported earlier [11,16]. For example, the ionic conducting glass–ceramics from the lithium aluminium titanium phosphate (LATP) system, when doped with Al_2O_3 and $AlPO_4$, form Al_2O_3:Li^+ and $AlPO_4$:Li^+ complexes which are unstable above 70 °C. However, the BN:Li^+/$BETI^-$ and Li_2O:Li^+/$BETI^-$ complexes show no evidence of instability around 70 °C. For example, the conductivity should have decreased if the BN:Li^+/$BETI^-$ had decomposed into BN and Li^+/$BETI^-$ (Eq. (iii) proceeding leftward). Similarly, the conductivity

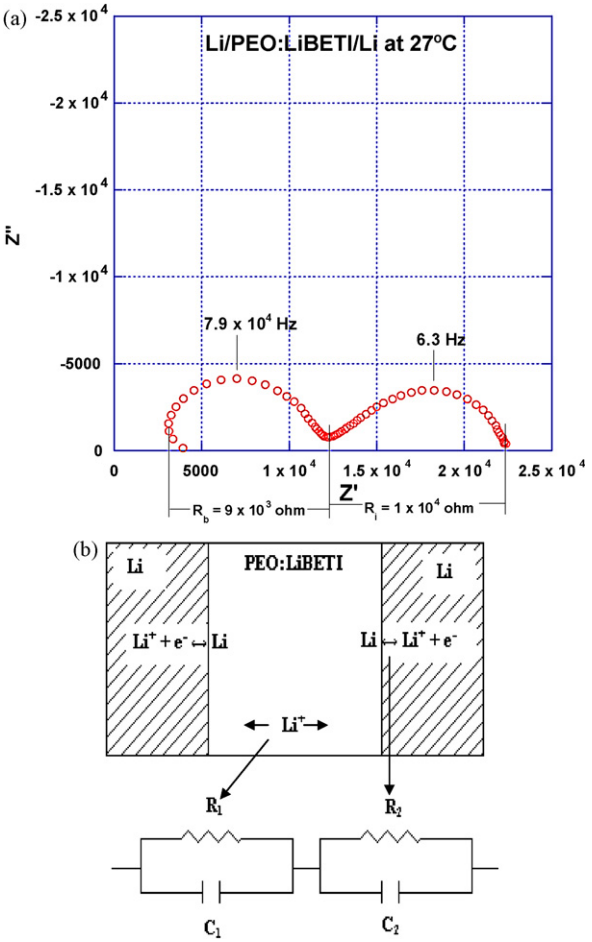

Fig. 4. Nyquist plots of (a) Li/PEO:LiBETI/Li cell at 27 °C just after cell assembly and (b) equivalent circuit of a Li/PEO:LiBETI/Li cell.

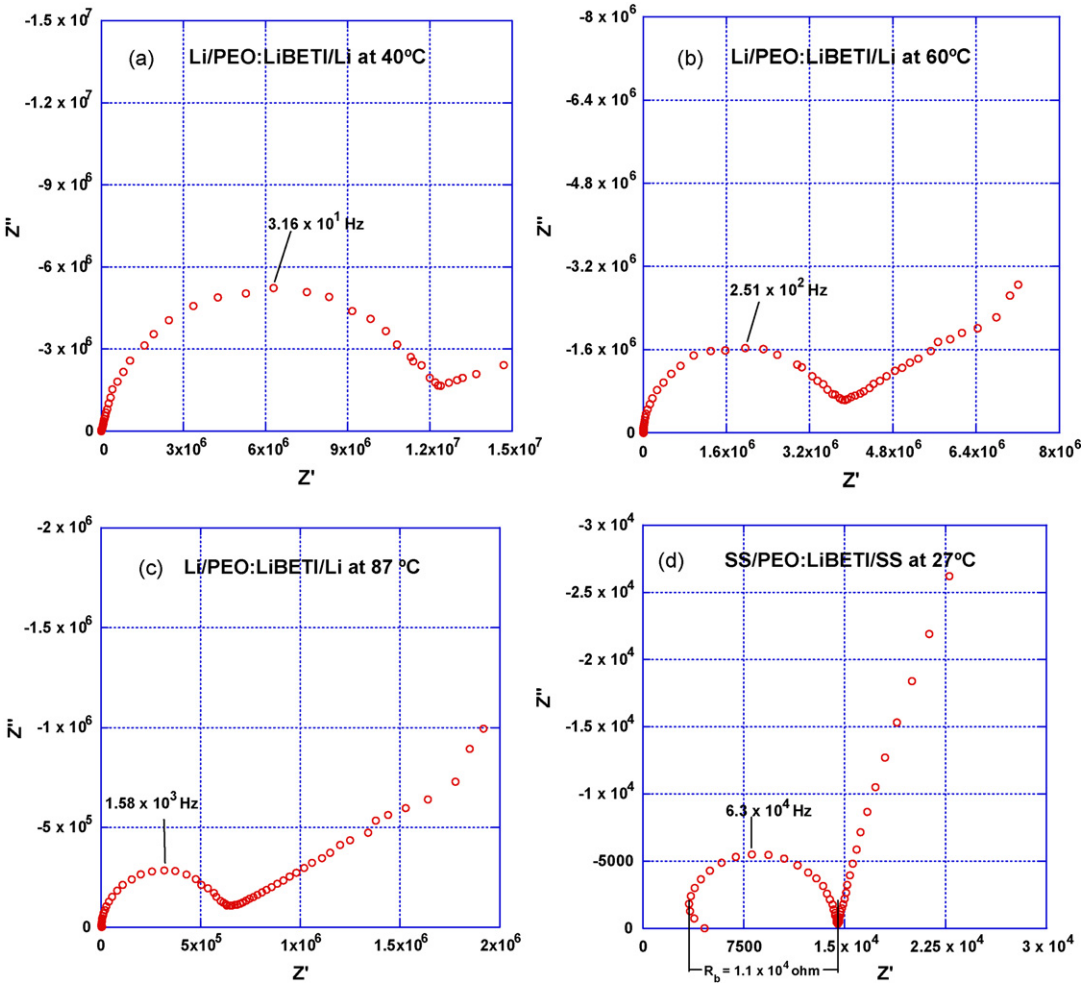

Fig. 5. Nyquist plots of Li/PEO:LiBETI/Li cell at (a) 40, (b) 60, (c) 87 °C after storage of the cell at room temperature for 552 h of cell assembly, and (d) Nyquist plot of the SS/PEO:LiBETI/SS cell after its assembly.

should also have decreased if the $Li_2O{:}Li^+/BETI^-$ had decomposed into Li_2O and $Li^+/BETI^-$ (Eq. (iv) proceeding leftward).

3.2. AC impedance with non-blocking (lithium) electrodes

The Nyquist plot from a Li/PEO:LiBETI/Li cell is shown in Fig. 4(a). The plot in Fig. 4(a) shows two semicircles: the first centered around 7.9×10^4 Hz and the second one at 6.3 Hz. An equivalent circuit representing the cell is shown in Fig. 4(b). The equivalent circuit is composed of two subcircuits. The first subcircuit consists the electrolyte resistance, R_1 and capacitance, C_1 and the collective contribution of R_1 and C_1 leads to a semicircle in the high frequency region (7.9×10^4 Hz) of the Nyquist plot. The second subcircuit consists of the charge-transfer resistance, R_2 and the capacitance, C_2. This subcircuit also yields a semicircle in the Nyquist plot at low frequency (6.3 Hz). Since both the circuit elements are perpendicular to the direction of current, they are connected in a series according to the practice reported in literature [17]. The charge-transfer reaction is expressed by Eq. (v).

$$Li \Leftrightarrow Li^+ + e^- \quad (v)$$

After the Li/PEO:LiBETI/Li cell was aged for 552 h at ambient temperature, the AC impedance measurement was repeated. The impedance data of the Li/PEO:LiBETI/Li cell in the form of the Nyquist plots at 40, 60, and 87 °C are shown in Fig. 5(a–c), respectively. All these figures show only one semicircle with very high resistance—7×10^5–1.2×10^7 Ω. The semicircles are followed by an almost 45° spike at low frequencies, which is related to the electrode process. The electrolyte resistance as measured by the blocking electrode technique was about 11,362 Ω at 27 °C (Fig. 5(d)). Fig. 5(a) shows a resistance of about 1.2×10^7 Ω of the cell at 40 °C, implying that it represents the sum of the electrolyte and charge-transfer resistances. Apparently, the charge-transfer resistance, R_2, is much greater than the electrolyte resistance, R_1. Therefore, the semicircle representing R_1 is masked by the massive semicircle resulting from the charge-transfer resistance, R_2. As cell storage time at ambient temperature increased, interface resistance became so large that the two semicircles merge into one semicircle. The resistance of the cell and hence its conductivity is dominated by the charge-transfer resistance.

The AC impedance spectra of the Li/PC(BN)/Li cell (after 552 h of cell storage at 23 °C) at 0, 14, 27, 40 and 87 °C are shown in Fig. 6(a–e), respectively. All these spectra display a wide variation in the semicircle shapes in the 10^6–0.1 Hz frequency range. Nonetheless, it is noted that 1 wt% of nanosize BN in the PEO:LiBETI matrix has led to much-reduced cell resistance and the cell reactions are shown by the existence of at least three semicircles. These three semicircles are evident in Fig. 6(b and c). In Fig. 6(b) the first semicircle is centered around 5.01×10^3 Hz, the second semicircle around 2.51×10^1 Hz, and the third semicircle at 2×10^{-1} Hz. With the increase in temperature to 40 °C, Fig. 6(d), two semicircles (intermediate and low frequencies)

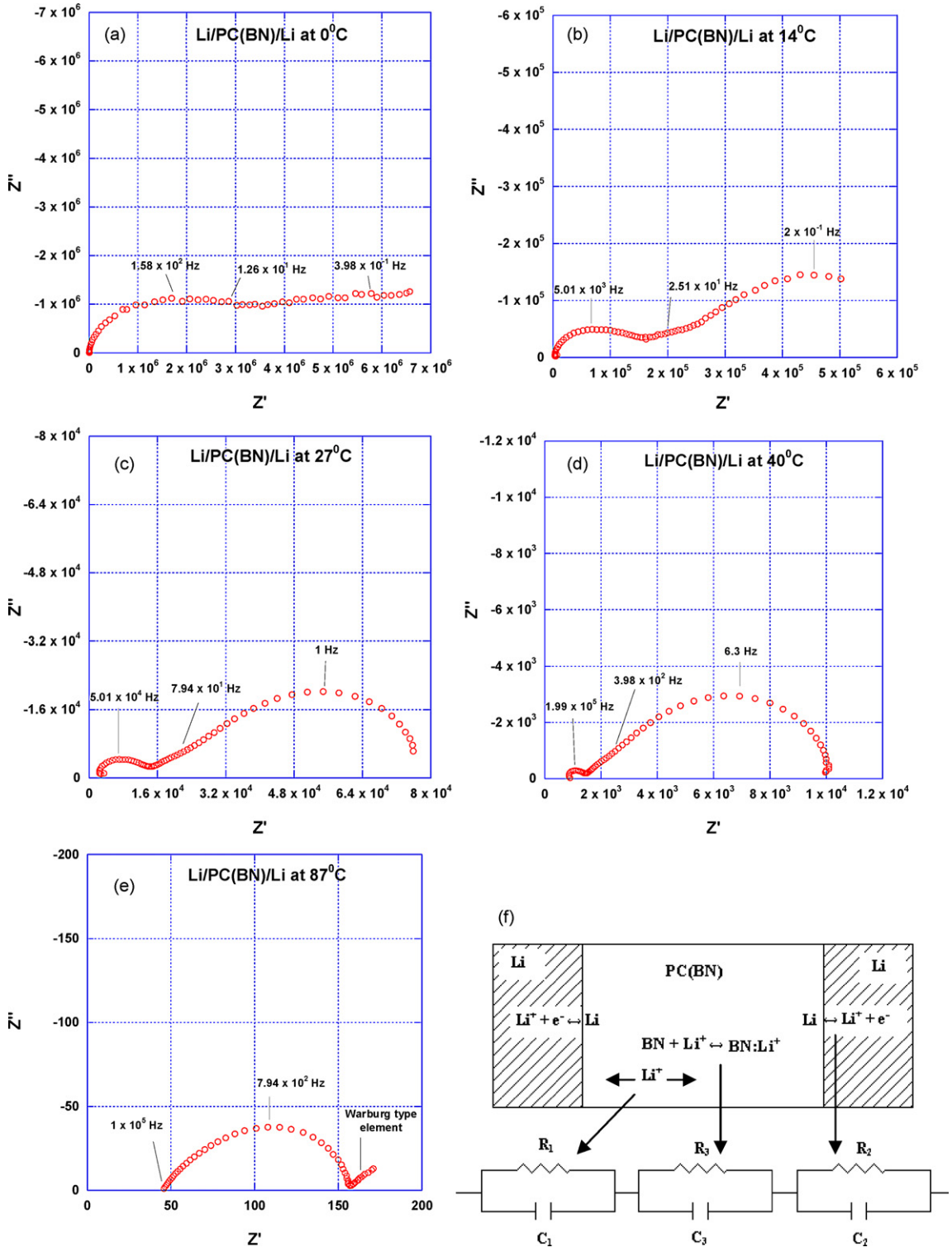

Fig. 6. Nyquist plots of a Li/PC(BN)/Li cell at (a) 0, (b) 14, (c) 27, (d) 40, (e) 87 °C after 552 h of aging at room temperature, and (f) equivalent circuit of a Li/PC(BN)/Li cell.

merge into a single asymmetric semicircle in the 10^2–0.1 Hz range. At higher temperature, 87 °C (Fig. 6(e)) only one asymmetric semicircle is observed. The electrode effect is shown by the Warburg type element at low frequencies in Fig. 6(e). The electrolyte or bulk resistance is related to the first and high frequency (5.01×10^3 Hz) semicircle of Fig. 6(b–e). The semicircles were resolved by the software available with the Solartron instrument. The cell resistance is the sum of the diameters of the three semicircles which was used to calculate the cell conductivity.

An equivalent circuit depicting electrochemical processes is shown in Fig. 6(f). Again in this case, the cell elements representing the chemical phenomena are perpendicular to the flow of current and are connected in series [17]. The bulk resistance for the transport of lithium ion is shown by a combination of resistor, R_1 and capacitor, C_1 and related by the first semicircle of the

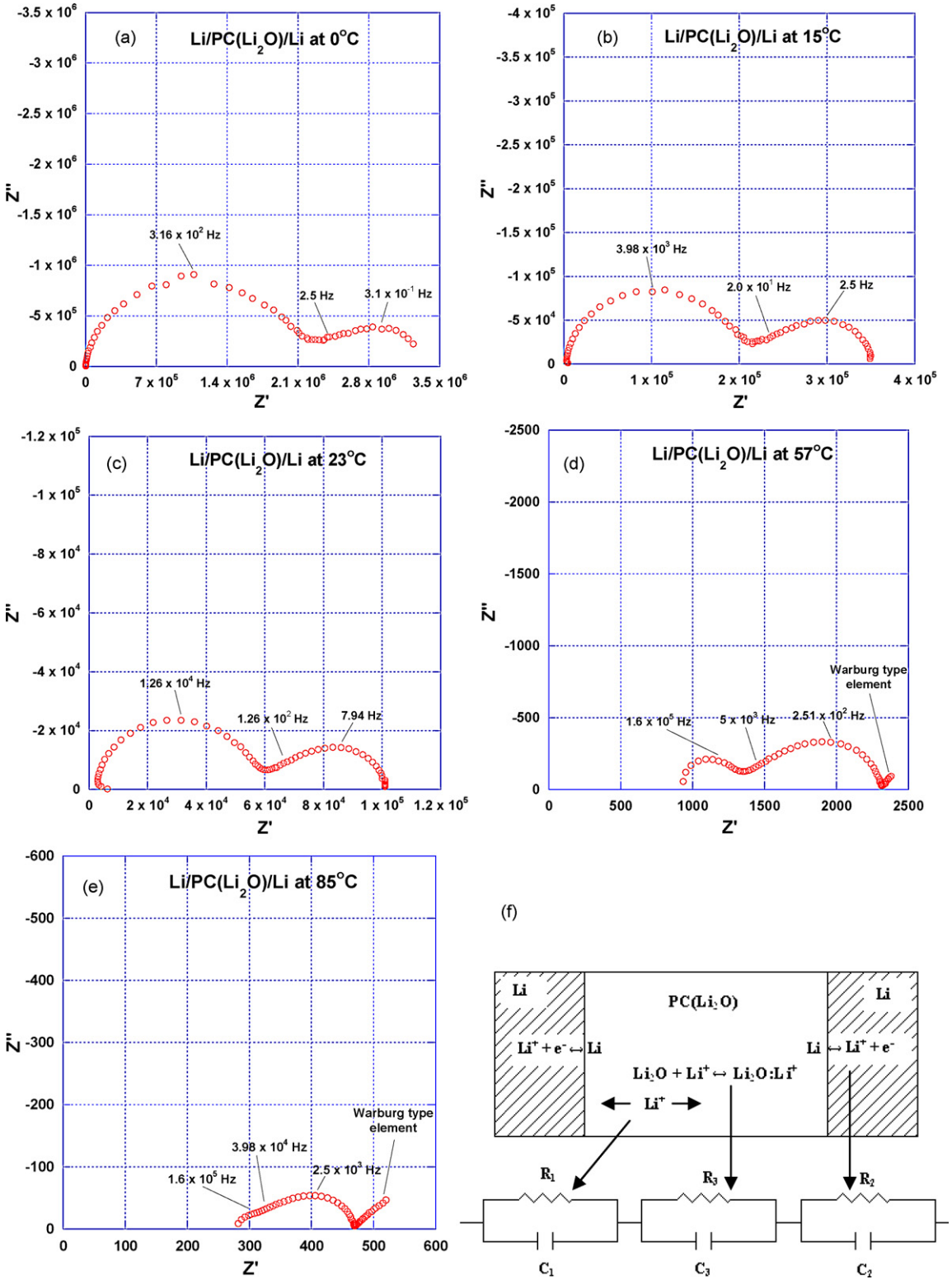

Fig. 7. Nyquist plots of a Li/PC(Li_2O)/Li cell at (a) 0, (b) 15, (c) 23, (d) 57, (e) 87 °C after 648 h of aging at room temperature, and (f) equivalent circuit of a Li/PC(Li_2O)/Li cell.

impedance data of Fig. 6(b). The formation of the BN:Li^+/$BETI^+$ complex as expressed by Eq. (iii) is again shown by a combination of resistor, R_3 and capacitor, C_3 and is proposed to be related to the second semicircle of Fig. 6(b). The charge-transfer reaction which was presented in Eq. (v) is shown by the combination of resistance, R_2 and capacitance, C_2 and relates to the third semicircle of Fig. 6(f).

The charge-transfer resistance was reduced by orders of magnitude by the addition of BN in the PEO:LiBETI matrix. For example, by comparing Figs. 5(c) and 6(e), both spectra obtained at 87 °C, shows an estimated reduction in charge-transfer resistance by about three orders of magnitude. The reduction suggests that it may have originated from the existence of the BN:Li^+/$BETI^+$ complex. Alternatively, the reduction in the charge-transfer resistance may have resulted

from the interface-mediated reaction. A similar effect in a composite electrolyte of PEO:$LiBF_4$ doped with lithium borosulfate glass has been reported earlier [18]. The charge-transfer resistance of the Li/composite electrolyte/Li cell decreased by a factor of three due to the incorporation of the ionic conducting glass in the PEO:$LiBF_4$ matrix. The cyclic voltammetry also revealed significant variation in the anodic and cathodic peak potentials and currents as the composition of the composite electrolyte was varied.

The AC impedance spectra of the Li/PC(Li_2O)Li cell (after 648 h of cell storage at room temperature) at 0, 15, 23, 57 and 87 °C are shown in Fig. 7(a–e), respectively. Each of these spectra also displays a wide variation in the semicircle shapes in the 10^6–0.1 Hz frequency range similar to Li/PC(BN)/Li cell. Also, 1 wt% of Li_2O in the PEO:LiBETI matrix has led to much reduced cell resistance as compared to Li/PEO:LiBETI/Li cell, and the cell reactions are shown by the existence of at least three semicircles. These three semicircles are evident in Fig. 7(a). In Fig. 7(a), the first semicircle is centered around 3.16×10^2 Hz, the second semicircle around 2.5 Hz, and the third semicircle at 0.31 Hz. With the increase in temperature to 57 °C, Fig. 7(d), intermediate and low frequency semicircles merge into a single asymmetric semicircle in the 10^5–10^2 Hz range. At higher temperature, 85 °C (Fig. 7(e)), only one asymmetric semicircle is observed. The electrode effect is shown by the Warburg-type element at low frequencies in Fig. 7(d and e). The electrolyte resistance is related to the first and high frequency (3.16×10^2–1.26×10^4 Hz) semicircle of Fig. 7(a–d). The cell resistance is the sum of the diameters of the three semicircles which was used to calculate the cell conductivity.

An equivalent circuit depicting electrochemical processes is shown in Fig. 7(f). The bulk resistance for the transport of lithium ion is shown again by a combination of resistor, R_1 and capacitor, C_1 and related by the first semicircle of the impedance data of Fig. 7(a–e). The formation of the Li_2O:Li^+/$BETI^-$ complex as expressed earlier by Eq. (iv) is again shown by a combination of resistor, R_3 and capacitor, C_3 and is proposed to be related to the second semicircle of Fig. 7(a–e). The charge-transfer reaction which was presented earlier by Eqs. (v) is shown by the combination of resistance, R_2 and capacitance, C_2 and relates to the third semicircle of the Fig. 7(a–e).

A comparison of Figs. 6(a–e) and 7(a–e) reveals that BN is more effective in reducing electrolyte resistance, whereas the Li_2O is superior in reducing the charge-transfer resistance. For example, if one compares the relative size of the semicircles in Figs. 6(a–e) and 7(a–e), the prior statement is justified. However, the temperature dependences of these two resistances (electrolyte and charge-transfer) are different which will be explained later.

In the case of Li_2O-containing electrolyte, the charge-transfer resistance was also reduced by at least three orders of magnitude. The experimental observation is explained on the basis of catalytic effects arising from the existence of Li_2O:Li^+ complex present in the PC and near Li-PC interface.

3.3. The electrolyte and cell conductivities

Fig. 8 presents the electrolyte and cell conductivities obtained from the cells using non-blocking lithium electrodes. These cells were aged for 552 h in case of Li/PEO:LiBETI/Li and Li/PC(BN)/Li) cells and 648 h for the Li/PC(Li_2O)/Li cell at ambient temperature. The Arrhenius plot of cell conductivity from the Li/PEO:LiBETI/Li cell show very low conductivity, less than 10^{-8} S cm^{-1} around 40 °C with an activation energy of 0.65 eV, Fig. 8(a). The Arrhenius plots of cell conductivities using PC(Li_2O) and PC(BN) electrolytes are shown in Fig. 8(b). Both plots show a transition around 58 °C. The reduced cell conductivity results from a large reduction in the charge-transfer resistance. The low temperature (<58 °C) activa-

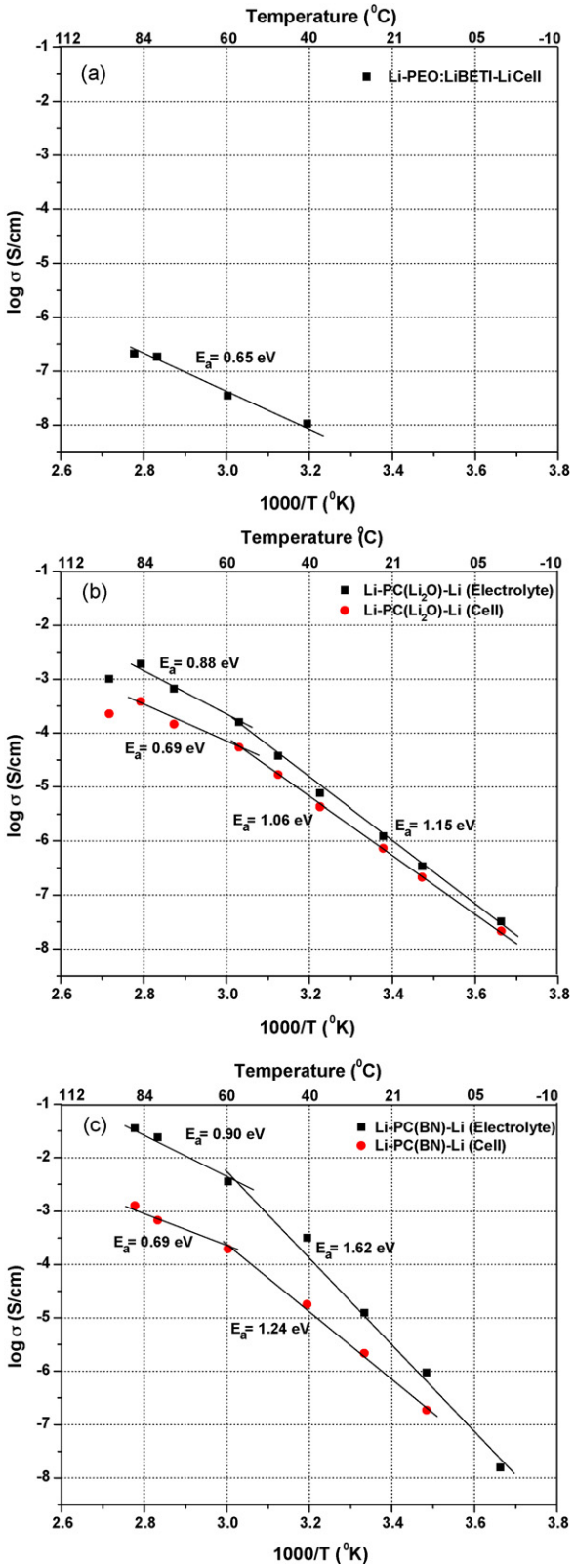

Fig. 8. Arrhenius plots of aged cells (a) Li/PEO:LiBETI/Li cell, (b) Li/PC(BN)/Li electrolyte and cell after 552 h of cell assembly, and (c) Li/PC(Li_2O)/Li cell and electrolyte after 648 h of cell assembly.

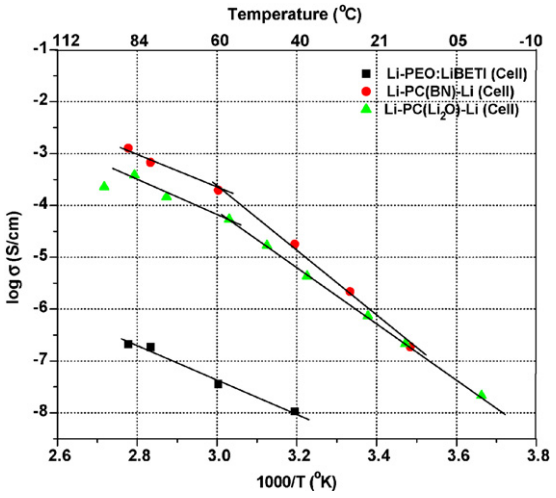

Fig. 9. Temperature-dependent comparison of Li/PEO:LiBETI/Li, Li/PC(BN)/Li and Li/PC(Li_2O)/Li cell conductivities.

tion energies are similar 1.06 and 1.15 eV. The high temperature activation energies show significant differences 0.69 vs. 0.88 eV. However, since the data represents a narrow temperature range (58–84 °C), any interpretation of the difference should be deferred. It was also observed that the electrolyte and cell conductivities of Li/PC(Li_2O)/Li cell start decreasing above 84 °C as shown in Fig. 8(b), which is being investigated. The conductivities of the PC(BN) electrolyte and the cell are shown in Fig. 8(c). There is a larger difference in the electrolyte and cell conductivities as compared to the PC(Li_2O) electrolyte. The low and high temperature activation energies are similar.

A comparison of conductivities of cells containing PEO:LiBETI, PC(BN) and PC(Li_2O) is presented in Fig. 9. It is evident from the figure that the incorporation of BN and Li_2O enhances the long-term cell conductivity and is very useful for making electrochemical devices. Further comparison of conductivities of cells containing PEO:LiBETI, PC(BN) and PC(Li_2O) reveal that Li/PC(Li_2O)/Li cell possess higher conductivity in the low temperature region, whereas the Li/PC(BN)/Li cell has higher conductivity in the high temperature region. This implies that the Li/PC(Li_2O)/Li cell can be useful at lower temperature, whereas the Li/PC(BN)/Li cell can be advantageous at higher temperatures. Improvement in cell stability can be attributed to the formation of a protective layer on the lithium surface involving BN and Li_2O. The characteristics of the SEI layer will be investigated in a future study.

4. Summary and conclusions

The PEO:LiBETI-BN and PEO:LiBETI-Li_2O PC composite formulations were optimized to achieve higher conductivities, reduce charge-transfer resistance, and stabilize the SEI at the lithium anode. These optimized formulations are currently used to fabricate lithium–oxygen/air cells in our laboratory. The dielectric additives, BN and Li_2O, were found to be effective in enhancing interface-mediated lithium ion transport. Both BN and Li_2O were also found to possess a catalytic effect in reducing charge-transfer resistance by three orders of magnitude. Because of the BN and Li_2O additive, the long-term cell stability improved. We attribute this improvement to the formation of a passivating layer on the lithium surface. Temperature-dependent cell behavior indicates that BN is more effective in higher temperature cell operation, whereas Li_2O is more advantageous for lower temperature cell functioning.

Acknowledgement

Authors gratefully acknowledge the financial support by the Air Force Research Laboratory, Propulsion Directorate, under Contract No. FA 8650-04-D-2403, DO 10.

References

[1] C.C. Liang, J. Electrochem. Soc. 1210 (1973) 1289.
[2] K. Shahi, J.B. Wagner, Solid State Ionics 3 (4) (1981) 295.
[3] T. Jow, J.B. Wagner, J. Electrochem. Soc. 126 (1979) 1963.
[4] K. Hariharan, J. Maier, J. Electrochem. Soc. 142 (1995) 3469.
[5] B. Kumar, S.J. Rodrigues, L.G. Scanlon, J. Electrochem. Soc. 148 (10) (2001) A-1191.
[6] R.C. Agrawal, R.K. Gupta, J. Mater. Sci. 34 (1999) 1131.
[7] A. Mikrajuddin, G. Shi, K. Okuyama, J. Electrochem. Soc. 147 (2000) 3157.
[8] P. Knanth, J. Electroceram. 5 (2000) 111.
[9] B. Kumar, C. Chen, C. Varanasi, J.P. Fellner, J. Power Sources 140 (1) (2005) 12.
[10] J.S. Thokchom, C. Chen, K.M. Abraham, B. Kumar, Solid State Ionics 176 (23–24) (2005) 1887.
[11] B. Kumar, S. Nellutla, J.S. Thokchom, C. Chen, J. Power Sources 160 (2) (2006) 1329.
[12] B. Kumar, N. Gupta, Jitendra Kumar, J.P. Fellner, S.J. Rodrigues, Proceeding of the 43rd Power Sources Conference, Philadelphia, PA, USA, 7–10 July, 2008, p. 35.
[13] B. Kumar, Jitendra Kumar, The 3rd International Conference on Electroactive Polymers, Jaipur, India 12–18 October, 2008.
[14] B. Kumar, D. Thomas, Jitendra Kumar, J. Electrochem. Soc. 156 (7) (2009) A506.
[15] K.M. Abraham, Z. Jinag, B. Carroll, Chem. Mater. 9 (9) (1997) 1978.
[16] B. Kumar, J.S. Thokchom, J. Amer. Ceram. Soc. 90 (10) (2007) 3323.
[17] Y. Kato, S. Yokoyama, T. Yabe, H. Ikuta, Y. Uchimoto, M. Wakihara, Electrochem. Acta 50 (2004) 281.
[18] B. Kumar, J.D. Schaffer, M. Nookala, L.G. Scanlon, J. Power Sources 47 (1994) 63.